An Acad Bras Cienc (2022) 94(Suppl. 4): e20210946 DOI 10.1590/0001-3765202220210946
Anais da Academia Brasileira de Ciências | *Annals of the Brazilian Academy of Sciences*
Printed ISSN 0001-3765 I Online ISSN 1678-2690
www.scielo.br/aabc | www.fb.com/aabcjournal

GEOSCIENCES

Assessing Remotely Piloted Aerial Systems in the characterization of rocky shores for oil spills environmental sensitivity mapping, northern São Paulo littoral, Brazil

RODRIGO I. CERRI, FLÁVIO H. RODRIGUES, GABRIEL H.S. DE OLIVEIRA, FÁBIO A.G.V. REIS, ARTHUR WIECZOREK, GEORGE A. LONGHITANO & DÉBORA M. DUARTE

Abstract: The Environmental Sensitivity Index (ESI) for oil spills was developed to assist coordinators to evaluate oil spill impact along shorelines and also to coordinate the allocation of resources during and after the incident, aiming to reduce environmental damage and consequences. Recently, Remotely Piloted Aerial Systems (RPAS) are being used in a wide range of areas, since they complement traditional remote sensing data (e.g., satellite images) and offer a rapidly, precise, detail and high-resolution images that fit well for environmental studies. Herein, the use of high-resolution RPAS images for ESI analysis of rocky shores in the Brazilian territory was performed. Using RPAS images, with their higher-resolution compared with ArcGIS Pro Basemap satellite images, increased the detailed of ESI analysis for oil spills, increasing the number of regions in the rocky shore that are more sensitive to oil spills. The RPAS images were able to decrease the number of areas that were less sensitive to oil spills, and increase areas that are more sensitive to oil spills. This increase is important, since they were not detected in the ESI analysis using conventional ArcGIS Pro Basemap satellite images. The RPAS images permit to delineate precisely rocky shores, improving ESI interpretation in rocky shores.

Key words: Environmental sensitivity index, oil spill, remotely piloted aerial systems, rocky shores.

INTRODUCTION

The implementation of tools and indexes to prevent and mitigate oil spills impact in marine and coastal environments is of interest for oil and gas companies and also for environmental authorities and for the society in general (Jensen et al. 1993, Gil-Agudelo et al. 2015). They seek to prevent and avoid potential damages caused by oil spills to the natural realm and also to the resources that are essential for human activity (economic and/or non-economic) (Gil-Agudelo et al. 2015). For these purposes, to avoid, prevent and mitigate oil spills damages to marine and non-marine organisms, the Environmental Sensitivity Index (ESI) maps are fundamental to prepare guidelines for contingency planning (Tri et al. 2015). According to Nelson & Grubesic (2021), the consequences of oil spills and their impact in the environment remains a challenge until these days, including the prediction and the evaluation of the environmental damages caused by oil spills, as well as the mitigation efforts and cleanup tatics. The preexisting knowledge about coastal resources and other information (i.e., ESI analysis), as a detailed characterization of a given coastal region, are capable to: (i) generate a faster response and, consequently, reduce potential damage, and (ii)

create an effective distribution and allocation of resources, activities and efforts focused on the protection and cleanup of an area (Santos & Andrade 2009, Kankara et al. 2016).

The concept of Environmental Sensitivity Index (ESI) was originally developed to assist spill-response coordinators to evaluate the impact of oil along shorelines, and to evaluate and assist the allocation of resources during and after the oil spill incident, reducing the environmental consequences (Jensen et al. 1990, 1998, Leiger et al. 2012). The ESI aims to help and prioritize the efforts in specific locations in order to reduce environmental consequences of oil spills, and also the placement and allocation of fundamental resources during the cleanup and mitigation works (Jensen et al. 1998). In this context, coastlines are especially sensitive to oil spills because these areas comprise estuaries, wetlands, coastal mangrove, freshwater swaps, tidal flats, coastal plains, rocky shores and beaches (Tri et al. 2015). The ESI maps, that have been used for decades since 1979 (Cowardin et al. 1979, NOAA 2002), must provide a concise resume of the coastal resources and environments that can be potentially in risk if an oil spill occurs in the region (Petersen et al. 2002, Leiger et al. 2012, Sowmya & Jayappa 2016). In other words, the ESI analysis is important to map the level/degree of environmental sensitivity to oil spills events (Petersen et al. 2002, Utomo et al. 2021) and should be always made before oil spills occur (Oydepo & Adeofun 2011, Utomo et al. 2021). The classical classification of ESI is given by Petersen et al. (2002), that describes it as a map that is an integral component of oil-spill contingency planning and response. Notwithstanding, the ESI is a scale that classifies coastal environments regions (in the case of this study, the rocky shores) according to the "degree" (usually an ESI value of 1 to 10) of sensitivity of a given environment to oil spills - when you assign a ESI value to a certain region, it is related to the level of sensitivity this region has to oil spills.

The environmental remote sensing can make the observation of large areas, at a given spatial and temporal resolution, more efficient and accurate (Klemas 2015, Mahdavi et al. 2018). Historically, they have been successfully used in a wide range of areas, like weather and hurricane prediction, coastal dynamics observation, pollution detection, coastal land cover, tidal wetlands, forest, agriculture and urban areas mapping (Klemas 2015). The traditional remote sensing, such as the satellites data, offers the coverage of wide areas with multispectral images and a great revisit time for, per example, environmental studies (Klemas 2015). However, for some applications (e.g., land-use and wetlands mapping, coastline characterization and delimitation, LIDAR bathymetry, and oil slicks and spills tracking), they lack spatial resolution, even with high spatial resolution satellite data available in the present-days (Klemas 2015).

The Remotely Piloted Aerial Systems (RPAS) or Unmanned Aerial Vehicles (UAVs) tend to complement the remote sensing technologies that are available today (Manfreda et al. 2018, Doughty & Cavanaugh 2019, Hardin et al. 2019, Nikolakopoulos et al. 2019, Odonkor et al. 2019, El Mahrad et al. 2020). In general terms, they are more user friendly than all the geoinformatics and remote sensing technologies, relatively cheaper, smaller, lighter and practical, and also offer an alternative to conventional platforms for high-resolution remote sensing data acquisition, with a lower cost and higher operational flexibility (Klemas 2015, Bayirhan & Gazioglu 2020). These RPAS vehicles can be applied in a diverse range of areas, that includes precision agriculture (Zhang & Kovacs 2012, Freeman & Freeland 2015), surveillance (Hodgson et al. 2016), 3D mapping (Nex & Remondino 2014), search and rescue (Waharte & Trigoni

2010), general scientific research (Bayirhan & Gazioglu 2020), meteorology (Bayirhan & Gazioglu 2020) and environmental monitoring that includes oil spills environmental sensitivity mapping (Cunliffe et al. 2016, Ball et al. 2017, Bayirhan & Gazioglu 2020). The necessity for a precise, flexible and low-cost system that offers a higher spatial resolution, temporal frequency and global accessibility, make the RPAS a great choice that satisfies these needs (e.g., Yang et al. 2013, Odonkor et al. 2019).

In this study, a comparison between the use of traditional remote sensing data (i.e., satellite images) and images from RPAS are presented for the characterization of rocky shores for oil spills environmental sensitivity mapping (ESI analysis), in the southeast coastal region of Brazil (northern littoral of São Paulo State), in Ubatuba and Caraguatatuba municipalities. This approach was adopted in order to: (i) understand if and when the RPAS images are made useful in areas difficult to access by land and/or in specific target areas; (ii) compare the results of rocky shore characterization obtained from traditional remote sensing data (satellite images) and images from RPAS; and (iii) see the limitations and potentials of the above-mentioned images in the ESI analysis.

MATERIALS AND METHODS

The studied areas comprise two rocky shores with difficult terrestrial and marine access (walking or boat) due to the dense vegetation ("Mata Atlântica" Rainforest) and rough seas. Two areas were properly imaged: Area 1 - a rocky shore in the continent (onshore area, Ubatuba municipality, locality commonly known as "Praia da Lagoa" Beach, southeast of Tabatinga locality); and Area 2 - rocky shores that surround an island (offshore area, Cocanha Island, Caraguatatuba municipality, Massaguaçu locality) (Figure 1). Located at the Serra do Mar mountain range, the studied area belongs to the Neoproterozoic Ribeira Orogen, that is characterized by a complex geological and geomorphological framework. Mainly, the lithotypes that occurred in the studied area are part of the Costeiro Complex (Neoproterozoic) and are characterized by gneiss, migmatite, migmatitic gneiss, anfibolite, granite, schists and quartzite with well-marked foliation (Hasui et al. 1978, Chieregati et al. 1982, Heilbron et al. 2004, Hasui 2012). The Ribeira Orogen is intensely marked by NE-SW strike that is mainly structured by gneissic foliation, shear and fault zones formed during the Gondwana assembly (Brasiliano Orogeny). In this context, the lithotypes of the studied rocky shores are characterized by granites with well-marked foliation, orthogneiss and magmatitic gneiss with well-marked foliations that are usually parallel to compositional layering.

This study was developed under the "Santos Project - Santos Basin Environmental Characterization", coordinated by PETROBRAS/CENPES.

To identified the differences between the RPAS and satellite images in terms of detailed and Environmental Sensitivity Index (ESI) interpretations for oil spills, image interpretation were performed following approximately the 1:2300 viewing scale for satellite image and RPAS images. It is important to emphasize that the RPAS images can give a scale of approximately 1:300/1:400.

The presence of pipelines (from offshore oil camps), a gas and oil distribution station and roads that connects other areas to the São Sebastião port, especially Caraguatatuba region, turns the understanding of remote sensing techniques and the mapping of environmental sensitivity for oils spills an important key for risk mitigation and possible cleanup efforts.

Figure 1. Location of the two studied areas in Caraguatatuba and Ubatuba municipalities, northern coast of São Paulo State. The studied areas are indicated with dashed rectangles - Cocanha Island (Caraguatatuba municipality) and Praia da Lagoa Beach rocky shore (Ubatuba municipality). The gray line indicates the municipal limits between Caraguatatuba and Ubatuba municipalities.

The remote sensing images used in this study comprises: (i) remote sensing satellite images extract from the ArcGIS Pro Basemap; (ii) and orthorectified RGB RPAS images, and (iii) Digital Surface Model (DSM) obtained from the RPAS. In ESI mapping, Google Earth Pro historical images are often used to help the ArcGIS Pro Basemap interpretations. For the Area 1, historical images from Google Earth Pro (August/2013, August/2018 and June/2020) were used. Images from Google Earth Pro from August/2016, September/2017, October/2018 and March/2020 were analyzed for Area 2. The Google Earth Pro images were little used: were used mainly when some rocky shore characteristics were confused with some human work or construction (as a way to clarify doubts about some characteristics of the image). The RPAS images for all analyzed areas were obtained in October 08, 2020.

ArcGIS Basemap images

The ArcGIS Pro Basemap is commonly used as a reference map on which users can overlay their own data from layers and better visualize the geographic information. These maps are a powerful tool for environmental interpretation, providing context for a work and allowing the user to produce multiple features, raster or web layers. In this work, Imagery Basemap from ArcGIS Pro was used in order to compare these images with RPAS images. The Imagery Basemap use as a source: Esri, Maxar, GeoEye, Earthstar Geographics, CNES/Airbus DS, USADA, USGS, AeroGRID, IGN and the GIS User Community. According to the ArcGIS platform, the Imagery Basemap (WGS84) provides one meter or better satellite and aerial imagery in some parts of the earth and a lower resolution satellite imagery around the globe. Generally, this Basemap includes: (i) 15m TerraColor Imagery at small and mid-scales (~1:591M down to ~1:72k) and (ii) 2.5m SPOT Imagery (~1:288k to ~1:72k).

Remotely piloted aerial systems (RPAS) images

The image acquisition carried out with the RPAS was done on October 10 2020. The RPAS RGB images were obtained using a Phantom 4 Advanced (quadcopter manufactured by DJI) equipped with a 20 megapixels sensor. The images were acquired using a RGB camera (FC6310 model), with focus length of 8.8 mm and 20 Mp. Flights were planned with the software DroneDeploy, an app which the user specify some parameters (area of interest, overlap percentage, flight height and ground sample distance) to configure the flight. The flight was performed in a single grid mode and low quality or fuzzy photos were deleted from the dataset. The flight and processing parameters are presented on Table I.

The captured images were processed using the Agisoft Metashape Professional v1.7.1. The average processing time was one hour, using a desktop with an AMD Ryzen 9 3900X 12-Core Processor at 3.79 GHz, 32 GB RAM, and NVIDIA GeForce RTX 2070 super GPU. The processing steps are described in Figure 2. The first step is image alignment which photo triangulation is performed; followed by the sparse cloud points generation and densification of this cloud to increase the number of points cloud and decreasing empty spaces; next step is the construction of a 3D model that represents faithfully the imaged area called digital surface model (DSM); Lastly occurs the images orthorectification, where the features were projected orthogonally with constant scale to produce the orthomosaic.

Environmental sensitivity index - ESI

The Environmental Sensitivity Index (ESI) mapping method currently in use in the Brazilian territory follows the guides of the Brazilian Ministry of the Environment ("Ministério do Meio Ambiente - MMA"; MMA 2004). The MMA (2004) is based on the National Oceanic and

Table I. Flight and processing parameters on October 10, 2020, using a Phantom 4 Advanced.

	Total area of flight (ha)	Total of images	Time of flight (min)	Overlap (%)		Ground resolution (cm/pix)
				Front	Side	
Praia da Lagoa Beach (Ubatuba/SP)	60	190	22	80	75	7.51
Cocanha Island (Caraguatatuba/SP)	11	162	12	85	80	3.23

Atmospheric Administration (NOAA 2002, Michel & Dahlin 1993), and give guidelines for developing ESI maps and databases in Brazil. In this method, rocky shores show highly variable situations where their physiographic attributes, and consequently their sensitive environmental conditions, give us their mobility and penetration for oil spills. In the MMA (2004) guidelines, 10 ESI classes for a wide range of coastal environments (Table II) are present. Table II shows some of the environments and their respective ESI: from the less sensitive environment (e.g., ESI 1) to the most sensitive environment (e.g., ESI 10).

Between the different ESI classes presented in the MMA (2004) guidelines (Table II), only four ESI classes can be used to map the sensitivity of rocky shores for oil spills (Table III). In this table, some of the geological and geomorphological characteristics of the rocky shores and granular materials that the MMA (2004) considers for ESI mapping and analysis are presented. According to the MMA (2004), the most preponderant geomorphological aspects to evaluate ESI are the substrate permeability and its declivity. It is also important to characterize the rocky environment, besides its declivity and permeability. The characterization and recognition of the rock type that compound the rocky shores and substrate and if they are autochthonous or allochthonous are also an important feature to be considered.

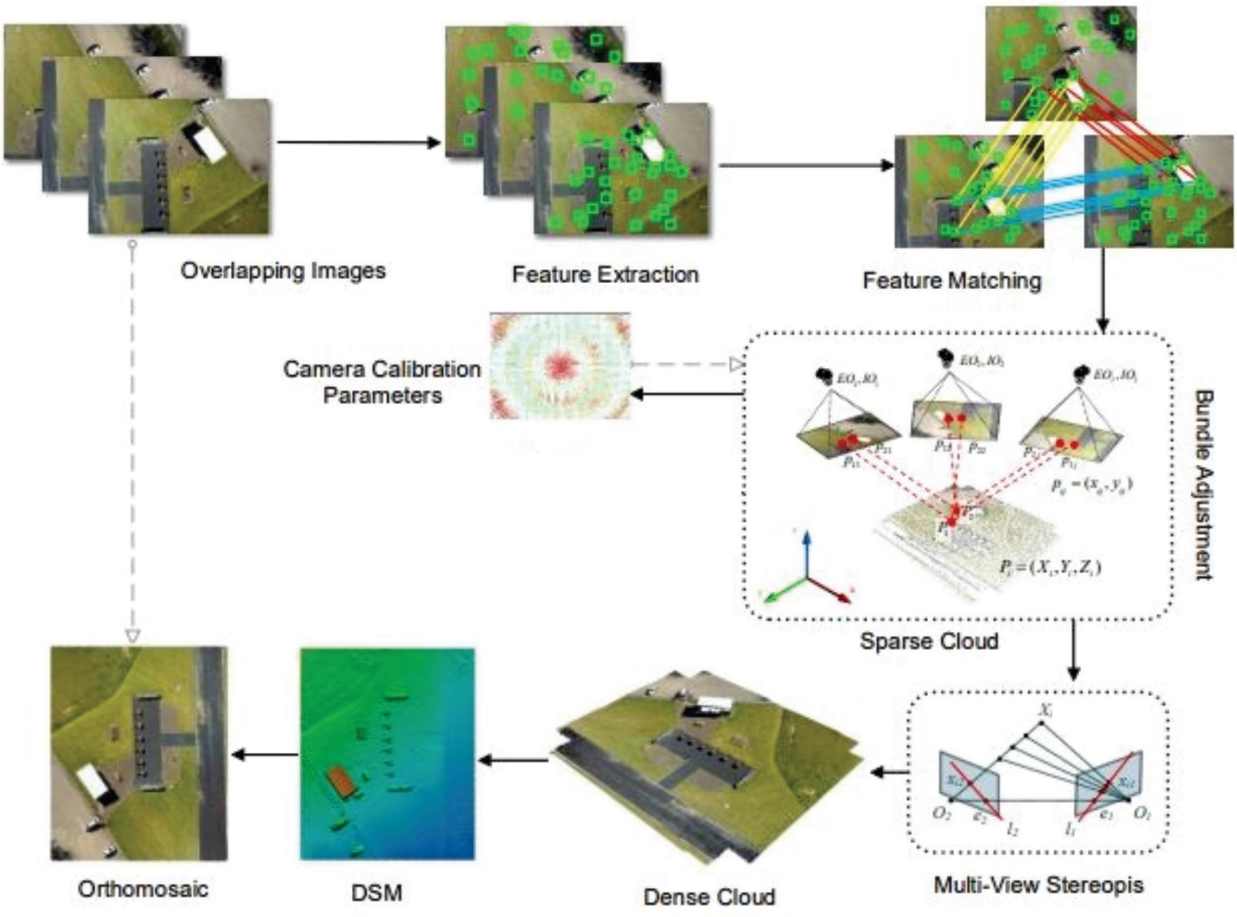

Figure 2. Flowchart of the photogrametry processing steps. Adapted from Javadnejad et al. (2021).

Table II. Environmental Sensitivity Index (ESI) classes following the guidelines proposed by the Brazilian Ministry of the Environment ("Ministério do Meio Ambiente - MMA"; MMA, 2004).

Environmental Sensitivity Index (ESI)	Shore type
ESI 1	Smooth rocky shores, high declivity, exposed
	Sedimentary rocks cliffs, exposed
	Smooth artificial structures, exposed
ESI 2	Smooth rocky shores, medium to low declivity, exposed
	Terraces or substrates with medium declivity, exposed
ESI 3	Dissipative beaches with fine to medium sand, exposed
	Contiguous sandy strips, not vegetated, subject to the action of stormy waves (isolated or multiple sand bars, "long beach")
	Steep cliffs and slopes
	Exposed dune areas
ESI 4	Beaches with coarse sand
	Intermediate beaches with fine to medium sand, exposed
	Beaches with fine to medium sand, sheltered
ESI 5	Mixed beaches with sand and gravel, shells and coral fragments
	Abrasion terrace or platform with irregular surfaces or covered by vegetation
	Fringed sand reefs
ESI 6	Gravel beaches
	Limestone detritus shore
	Talus deposits
	Rockfills (e.g., rip-rap), exposed
	Exhumed platform or terrace covered by lateritic concretions (porous or shapeless)
ESI 7	Sandy tidal plain, exposed
	Low water terrace
ESI 8	Smooth rocky scarp/slope, sheltered
	Fractured rocky scarp/slope, sheltered
	Sandy scarps and steep slopes, sheltered
	Rockfills (e.g., rip-rap), sheltered
ESI 9	Sandy/muddy tidal plain and other non-vegetated humid coastal areas
	Muddy low water terrace, sheltered
	Sandy reefs supporting corals
ESI 10	Deltas and vegetated river bars
	Wetlands, river and lagoons banks
	Brackish or salty water wetlands with vegetation adapted to these environments
	Everglades
	Mangroves

ESI photointerpretation criteria

The satellite and RPAS images were interpreted for ESI according to several parameters that follows the MMA (2004) method, which defines classification criteria correlating declivity, permeability and oil sensitivity to the aforementioned environments. The classification of the terranes where rocky shores, cobble/boulders camps and talus deposits occur in the selected areas (see Figure 1), were made considering the following parameters (Tables III and IV): (i) shore type; (ii) exposure to wave action; (iii) declivity; (iv) fracture degree; and (v) intertidal width. These parameters were analyzed together and classified in order to stablish a final Environmental Sensitivity Index (ESI) for oil spills. The declivity was obtained through the Digital Surface Model (DSM) provided by the RPAS mapping and imaging. It is worth noting that the guidelines from MMA (2004), uses a visual declivity analysis, leaving this parameter very subjective and subject to different interpretations depending on the person that is working with it.

Table IV shows the parameters classification, aiming the sensitivity for oil spills assessment for each analyzed rocky shore in the study areas, based on MMA (2004) proposal (Tables II and III). In general terms, observing the current ESI analysis, it is clear that rocky shores with lower values of declivity and high fractured degree tend to have a higher ESI than those with higher values of declivity and lower fractured degree.

RESULTS

ArcGIS pro basemap environmental sensitivity index

The aforementioned parameters were analyzed (see Section 2.3) for ESI for oil spills in two different areas using the satellite images from ArcGIS Pro Basemap. In terms of length of the rocky shores that corresponds to Area 1 and 2, they have, respectively, 2.312 km and 948 m.

After the analysis of the photointerpretative parameters (e.g., littoral and shore type, declivity, fracture degree, etc.), four ESI classes were recognized using the ArcGIS Pro Basemap images: ESI 1, ESI 2, ESI 6 and ESI 8. These ESI were observed in, respectively, 14, 9, 19 and 11 segments along the two analyzed rocky shores. The Figure 3 shows the two studied shore lines (Area 1 and 2) with their respective ESI classes that were identified by detailed analysis of ArcGIS Pro Basemap satellite images. Table V shows the number of segments in each class of ESI identified for both areas. Table VI show how much of this extension corresponds to each of the ESI classes identified in this study (sum of length of each mapped ESI segments), and the contribution (percentage) of each ESI class in the extension of the rocky shores.

For Area 1, where only three ESI classes were identified (Figure 3), it is observed that: (i) the ESI 1 appears 12 times along the rocky shores, corresponding to 42.2% of its extension; (ii) ESI 2 appears seven times along this rocky shore and represents only 18.5% of its extension; (iii) the ESI 6 appears in 14 segments along the rocky shore (910 m) and corresponds to 39.4% of the extensions of the analyzed rocky shore. On the other hand, observing Area 2, the most part of the area was classified as ESI 8, the most sensitive index in the current analysis, due to its location in sheltered waters. The ESI 8 corresponds to half of the mapped extension (54.2%) and appears in 11 segments along this rocky shore. Likewise, ESI 6 is an important value and relates to a quarter of the mapped extension (24.9%) Thus, using ArcGIS Pro Basemap satellite images, it is possible to see that: (i) for the Area 1, the rocky shores present greater variability of sensitivity indexes, mostly, ESI 1 and ESI 6 classes; and (ii) for the Area 2, the rocky shores are mostly composed by highly sensitive areas for oil spills (about 80%).

Table III. Geological and geomorphological characteristics of environments with rocky and granular substrate, according to the MMA (2004).

Littoral Type	Intertidal zones		Substrate Type	Environmental Sensitivity Index (ESI)
	Declivity (degrees)	Width (meters)		
Exposed rocky shores	> 30	Narrow	Rocky shore	1
Wave eroded platforms	< 30	Wide	Rocky bed	2
Gravel beaches	10 - 20	-	Gravel	6
Sheltered rocky shores	> 15	Narrow	Rocky bed (with some sediments)	8

Table IV. Photointerpretative criteria used in the ESI mapping in this study. These criteria followed the guidelines of MMA (2004).

Exposure to wave action	Shore type	Fracture degree	Declivity (degrees)	
			Sheltered environments	Exposed environments
Exposed	In-situ rock outcrop	Unfractured or low-fractured (smooth)	0 - 5 (flat)	0 - 5 (flat)
Sheltered	In-situ rock outcrop and cobbles/boulders	Medium to highly fractured (not smooth)	5 - 15 (low)	5 - 15 (low)
	Cobbles/Boulders		15 - 30 (high)	15 - 30 (medium)
	Talus deposits		> 30 (very high)	> 30 (high)

Remotely piloted aerial systems (RPAS) environmental sensitivity index

For the RPAS ESI analysis, the Area 1 presented 2.121 km of extension along the analyzed rocky shore. In this area, rocky shores are classified into three ESI classes: ESI 1, ESI 2 and ESI 6 in, respectively, five, 23 and 27 segments along the rocky shore (Figure 4, Table VII). For the Area 2, with 1.248 km of extension, four ESI classes were identified: ESI 1, ESI 2, ESI 6 and ESI 8 within, respectively, five, 11, 13 and 41 segments along the rocky shore (Figure 4, Table VII).

Comparing the images obtained by the RPAS imaging with the ArcGIS Pro satellite image, the RPAS images gave us a higher value of rocky shore length/extension. The RPAS images give the user the possibility to trace a more detailed line throughout the rocky shores (e.g., better and detailed coastline and indents tracing, etc.). This is mainly due the fact that the images derived from the RPAS have a higher resolution and detailed than those observed in conventional satellite images (e.g., ArcGIS Pro Basemap).

Analyzing the length of each ESI class (Table VIII) for Area 1, it is clear that ESI 2 is the most predominant class (1117 m of extension, 52.7%) followed by ESI 6 (910 m of extension, 42.9%). For Area 2, ESI 8 is the most representative class (708 m of extension, 56.7%) followed by approximately equal occurrences of ESI 2 and

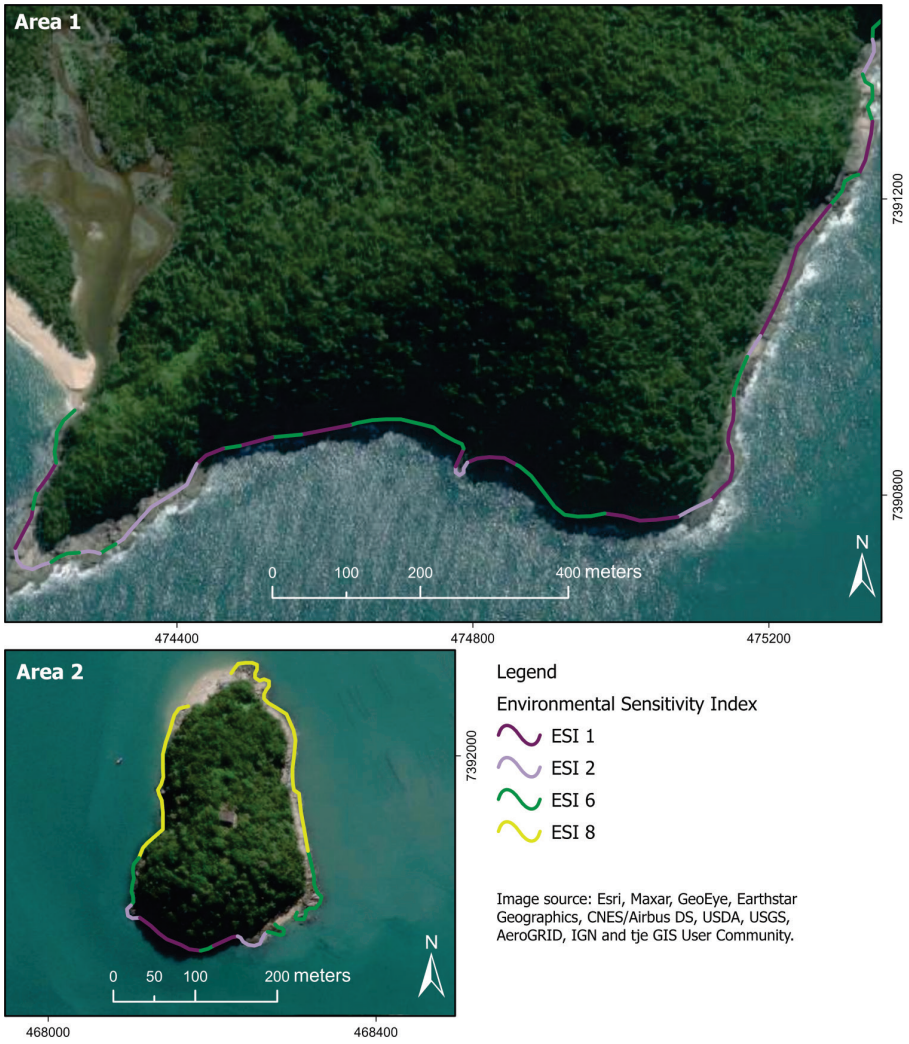

Figure 3. ArcGIS Pro Basemap satellite image with the interpreted Environmental Sensitivity Index (ESI) mapping for oil spills. Area 1 represents the "Praia da Lagoa" Beach rocky shore, and Area 2 represents Cocanha Island rocky shore.

ESI 6 (223 m and 198 m of extension, 17.9% and 15.9%, respectively).

Comparing the high-resolution RPAS images with the ArcGIS Pro Basemap satellite images, mainly five positive and interesting points in the use of these high-resolution images can be observed: (i) RPAS images offers a precise and detailed visual of fractures in the rocky shores; (ii) a precise knowledge up to where the sea level rises at high tide. With this, the identification of washing zones can be easily access (zones where waves interact with the rocky shores); (iii) a more nitid observation of regions where gravel and boulder occurred; (iv) RPAS images lack shadow zones (shadows from trees, for example), that often covers and hinders the identification of some areas when using ArcGIS Pro Basemap images; and (v) enables greater detail to define, delimit and recognize the limits of the rocky shores.

Table V. Number of segments observed in each ESI class, using ArcGIS Basemap satellite images for ESI mapping for oil spills.

	ArcGIS Pro Basemap satellite images									
	Environmental Sensitivity Index - ESI									
	1	2	3	4	5	6	7	8	9	10
Area 1	12	7				14				
Area 2	2	2				5		11		

Table VI. Table showing the total extension of each ESI class for Areas 1 and 2 and the corresponding percentage value of these in relation to the total length of the analyzed rocky shores extension. ESI values based on the ArcGIS Pro Basemap satellite images.

	ArcGIS Pro Basemap satellite images									
	Environmental Sensitivity Index - ESI									
	1	2	3	4	5	6	7	8	9	10
Area 1 (2.3 km)	975 m	427 m				910 m				
Percentage (%)	42.2	18.5				39.4				
Area 2 (948 m)	118 m	80 m				236 m		514 m		
Percentage (%)	12.4	8.4				24.9		54.2		

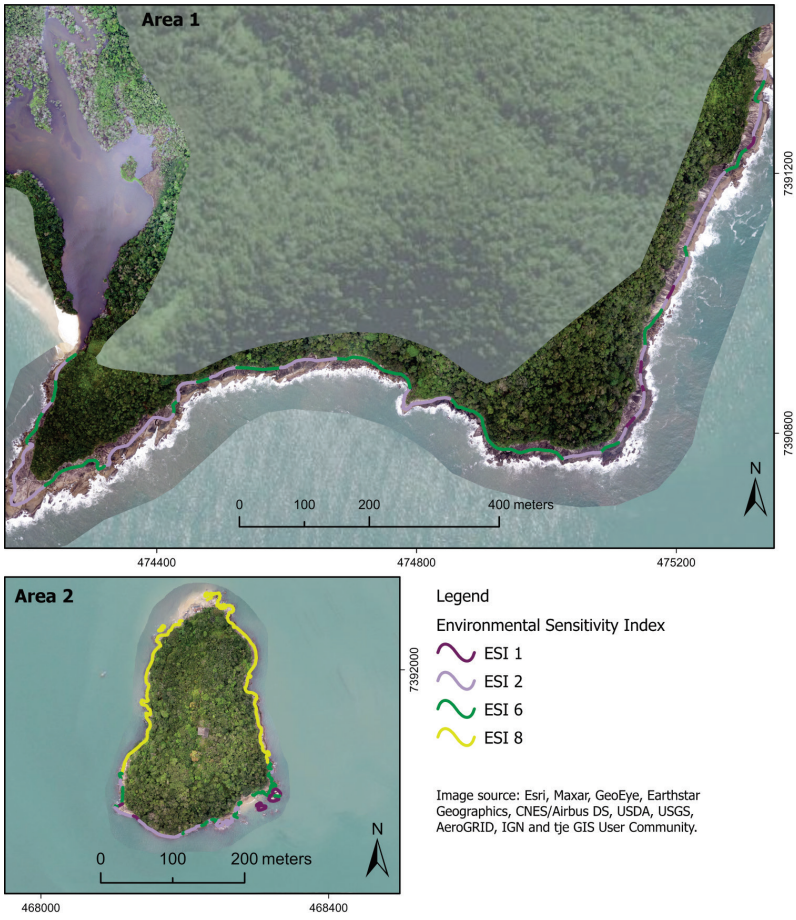

Figure 4. Remotely Piloted Aerial System (RPAS) high-resolution image with the interpreted Environmental Sensitivity Index (ESI) mapping for oil spills. Area 1 represents the "Praia da Lagoa" Beach rocky shore, and Area 2 represents Cocanha Island rocky shore.

Table VII. Number of segments observed in each ESI class, using Remotely Piloted Aerial Systems (RPAS) images for ESI mapping for oil spills.

	Remotely Piloted Aerial Systems (RPAS) images									
	Environmental Sensitivity Index - ESI									
	1	2	3	4	5	6	7	8	9	10
Area 1	5	23				27				
Area 2	5	11				13		41		

Table VIII. Table showing the total extension of each ESI class for Areas 1 and 2 and the corresponding percentage value of these in relation to the total length of the analyzed rocky shores extension. ESI values based on the Remotely Piloted Aerial Systems (RPAS) images.

	Remotely Piloted Aerial Systems (RPAS) images									
	Environmental Sensitivity Index - ESI									
	1	2	3	4	5	6	7	8	9	10
Area 1 (2.121 km)	94	1117				910				
Percentage (%)	4.4	52.7				42.9				
Area 2 (1.248 km)	119	223				198		708		
Percentage (%)	9.5	17.9				15.9		56.7		

DISCUSSIONS

ESI mapping for rocky shores: ArcGIS Pro Basemap versus RPAS images

The solely analysis of the quantity of ESI classes mapped within the studied areas (Figure 5a) shows a very interesting pattern. Comparing the quantity of ESI classes obtained interpretating the ArcGIS Pro satellite and RPAS images, the interpretation of satellite images tends to give us more areas with lower ESI values in the studied rocky shores (e.g., ESI 1). However, when analyzing the same areas using an image with higher resolution and detailed, like de RPAS images used here, the number of areas with ESI 1 decreases and the number of areas with higher sensitivity index (e.g., ESI 8) notably increases (Figure 5a). In the specific graph presented in Figure 5a, for the quantity of ESI classes for Area 1 and 2, the number of regions with ESI 8 increases almost four times using RPAS images, and the same pattern can be observed for the ESI 2 and ESI 6.

For Area 1, the use of RPAS imaged for ESI mapping and analysis was particularly interesting (Figure 5b). For the "Praia da Lagoa" Beach rocky shore (Area 1; see also Figures 3 and 4) the following characteristics worth mentioning: (i) the number of regions with ESI 1 decreased using RPAS images; (ii) the number of regions with ESI 2 increased from 7 (using ArcGIS Pro Basemap) to 23 using the RPAS images; and (iii) none of the images identified ESI 8 in this area. In this case, the use of RPAS images decreased the number of areas that were not too sensitive to oil spill (ESI 1) and almost double the number of areas that are more sensitive to oil spills (ESI 2 and ESI 6). At first, the high resolution and detailing of the RPAS images offered the opportunity to see features in the rocky shore that increases the number of regions with higher ESI classes.

The use of RPAS images versus ArcGIS Pro Basemap satellite images, in Area 2 (Cocanha Island rocky shore), gave interesting results too (Figure 5c). For all ESI classes mapped for this area, a notable and important increase in the number of ESI classes when using the RPAS images is observed (Figure 5c). Analyzing this area, the ESI classification increased tremendously between the satellite and RPAS images, especially regions with the highest sensitivity for oil spills (ESI 8; see also Figures 3 and 4). This is mainly due the higher resolutions of the RPAS images compared to the satellite images of the ArcGIS Basemap. The increase of regions classified as ESI 8 is interesting, once that these regions where underestimated when the same region were analyzed using satellite images.

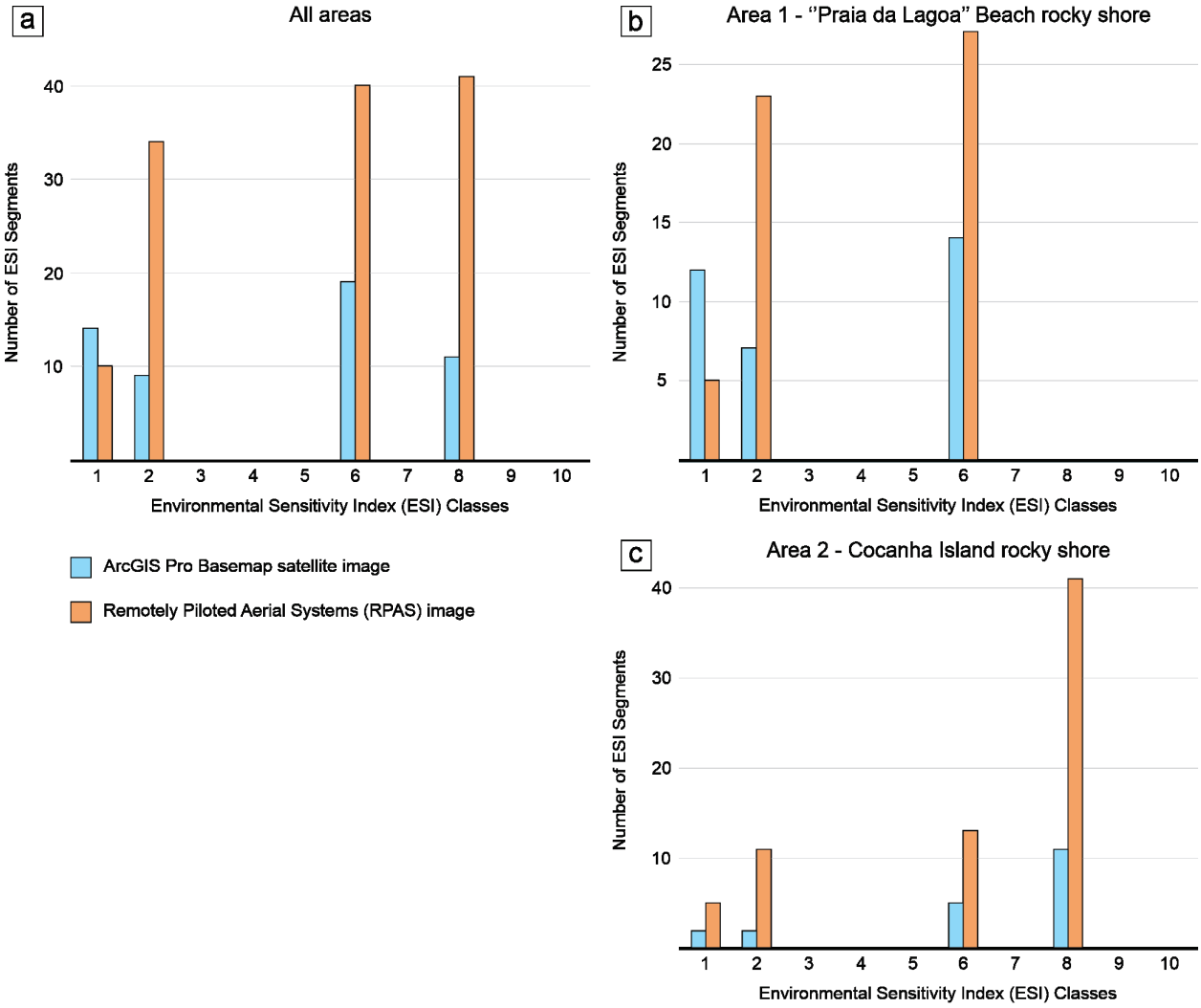

Figure 5. Bar graphs show the occurrence of regions with specific ESI values within the studies areas. (a) Occurrence of ESI values considering all the studied areas together. Occurrence of ESI values considering just (b) Area 1 ("Praia da Lagoa" Beach rocky shore) and (c) Area 2 (Cocanha Island rocky shore).

ESI length analysis: percentage distribution of ESI classes

The ESI length analysis was based on Tables VI and VIII, where the percentage of each ESI class was analyzed, considering the length of the entire rocky shores (Figure 6). This analysis mainly shows how much impact, with length, each of ESI class had on the entire analyzed rocky shores. It is important to emphasize that when the length of the studied rocky shore is observed (see Tables VI and VIII), the extension is always greater when ESI mapping is based on the RPAS images. This length difference is mainly due to the high resolution of RPAS images, allowing rocky shores interpretations to be more accurate and detailed (rocky shore trace and delineation is always more detailed in this high-resolution image).

For "Praia da Lagoa" Beach rocky shore (Area 1) (Figure 6a) the impact of using RPAS images can be understood. This high-resolution image, compared with ArcGIS Pro Basemap satellite image, are capable of identify areas with higher ESI and, consequently, more sensitive to oil spills. The ESI interpretation based on RPAS

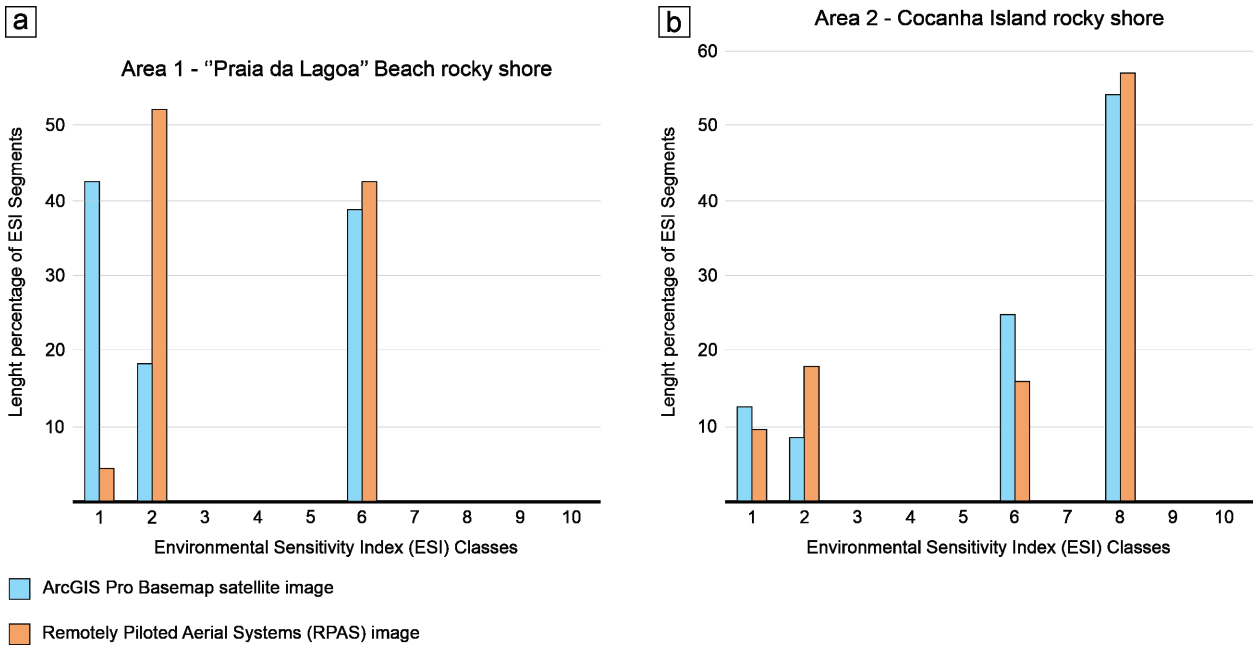

Figure 6. Percentage of ESI regions for Remotely Piloted Aerial Systems (RPAS) and ArcGIS Pro Basemap satellite images (a - Area 1, "Praia da Lagoa" Beach rocky shore; b - Cocanha Island rocky shore). Each bar on the graph represents a percentage of length (of the total length of the rocky shores) for each ESI class.

images mapped areas of greater extension (and in greater quantity) compared with the satellite images (Figure 6a). Using the RPAS images, it is possible to trace the notable decrease in the impact of regions with ESI 1, the notable increase in the impact of regions with ESI 2, and a little increase in regions with ESI 6.

In the Area 2, Cocanha Island, the interpretation difference, in terms of length, become very smooth (Figure 6b). Considering the length of each ESI class, the ESI mapping using both images are almost the same. In the RPAS image, there is the tendency in the decrease of regions with ESI 1 and ESI 6, while regions with ESI 2 increases. For regions with ESI 8, most sensitive to oil spills, their length is almost the same for both RPAS and ArcGIS Pro Basemap (Figure 6b).

The use of detailed RPAS images (and/or possibly other high-resolution images), causes more segmentation in the ESI interpretation, as can be seen in the increase and decrease of segments with certain ESI value. In other words, high-resolution images lead to a high segmented ESI interpretation. Taking into consideration contingency plans, RPAS images can be very useful, once they offered a high detailed mapping and a higher rocky shore ESI segmentation.

RPAS high resolution images for detailed ESI mapping

Observing the photointerpretative parameters used in this study for environmental sensitivity index analysis for oils spills, it is possible to identified the reasons why, using RPAS and ArcGIS Pro Basemap satellite images, regions with ESI 1 and ESI 2 always increase when using RPAS images. The standard analysis based on the Brazilian national guidelines for ESI studies (MMA 2004), using satellite images and other remote sensing products, suggests to use a visual declivity interpretation. In this sense, when using the methods and parameters

stablished by the MMA (2004), the declivity becomes a very interpretative parameter to be considered in the ESI.

Analyzing both ArcGIS Pro Basemap satellite and RPAS images, the interpretation of declivity varies greatly between them. The possibility to generate a Digital Surface Model (DSM) with the RPAS mapping raise the possibility to quantify precisely the declivity (Figure 7 and 8). In the Figure 7 ("Praia da Lagoa" Beach rocky shore), it is possible to observe that, with the precise values of declivity obtained from the RPAS DSM, the ESI in the rocky shores can be more detailed.

For example, in the rocky shore section shown in Figure 7a, it is possible, using the ArcGIS Pro Basemap satellite images, to interpret three ESI (ESI 1, ESI 2 and ESI 6). On the other hand, in this same section of Figure 7a, using RPAS images

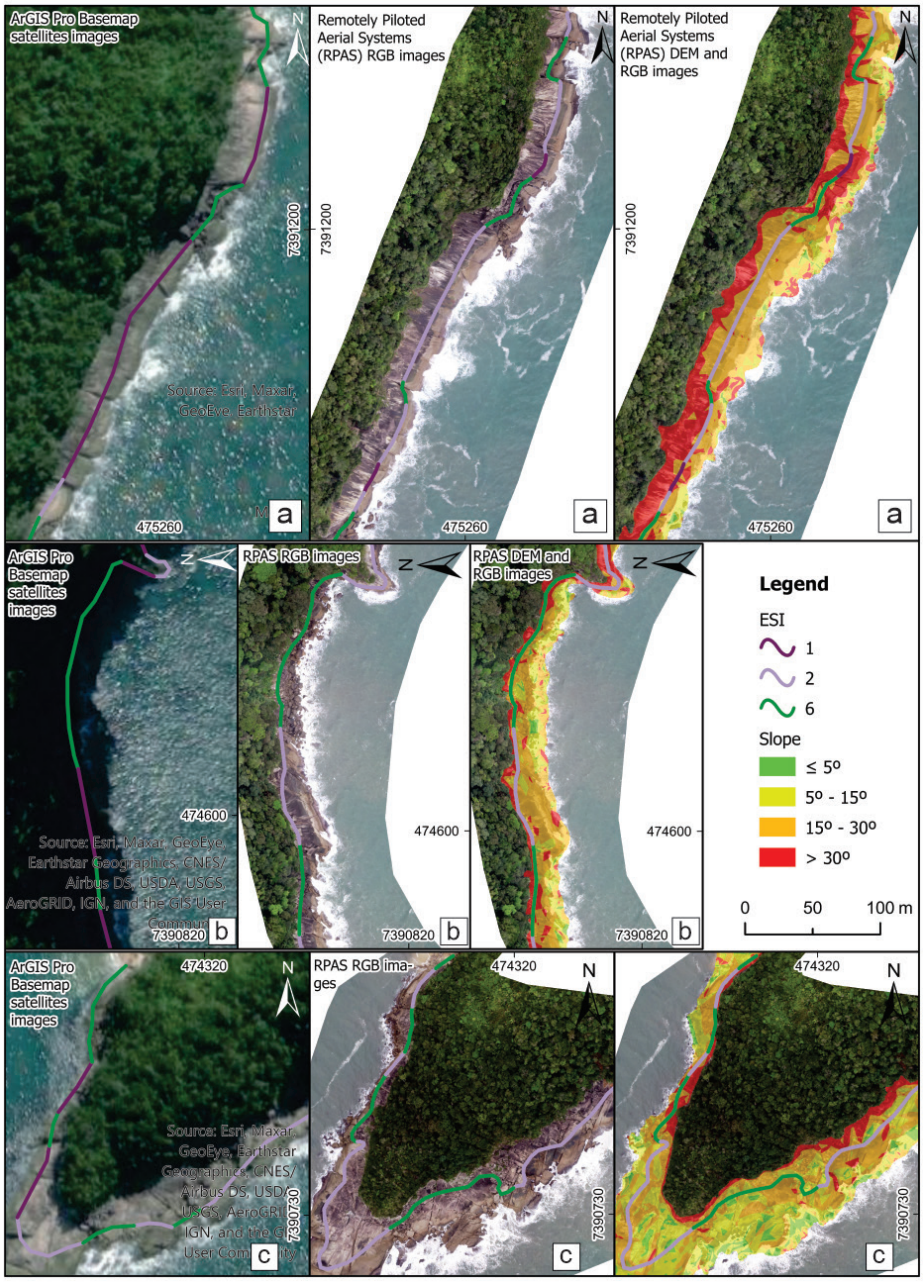

Figure 7. Interpreted ESI sections for the "Praia da Lagoa" Beach rocky shores. From the right to the left, images from the ArcGIS Pro Basemap satellite images, Remotely Piloted Aerial Systems (RPAS) images and RPAS Digital Surface Model (DSM) superimposed on RPAS high-resolution images. Colored lines are the interpreted ESI for the rocky shores. Observe that the number of ESI section increase when RPAS images are analyzed. Figures a, b and c shows different parts of the studied area with their respective ESI analysis and slope.

together with their DSM, the participation of regions with ESI 1 decreases and the number of sections with ESI 2 and ESI 6 increases. Thus, the use of RPAS images compartmentalized and detailed the mapped regions that were previously mapped using ArcGIS Pro Basemap satellite images. The same pattern is observed for the two other sections shown in Figures 7b and 7c. These changes, decreasing regions with ESI 1 and increasing regions with ESI 6 (see Figure 5, Tables V and VII), in interpreted mainly due: (i) the increase of image resolution and detail by using RPAS images; and (ii) the use of DMS images for the acquisition of precise declivity values.

For the offshore area, the Cocanha Island rocky shore, the same pattern can be noticed (Figure 8). In the Figure 8a, when observing

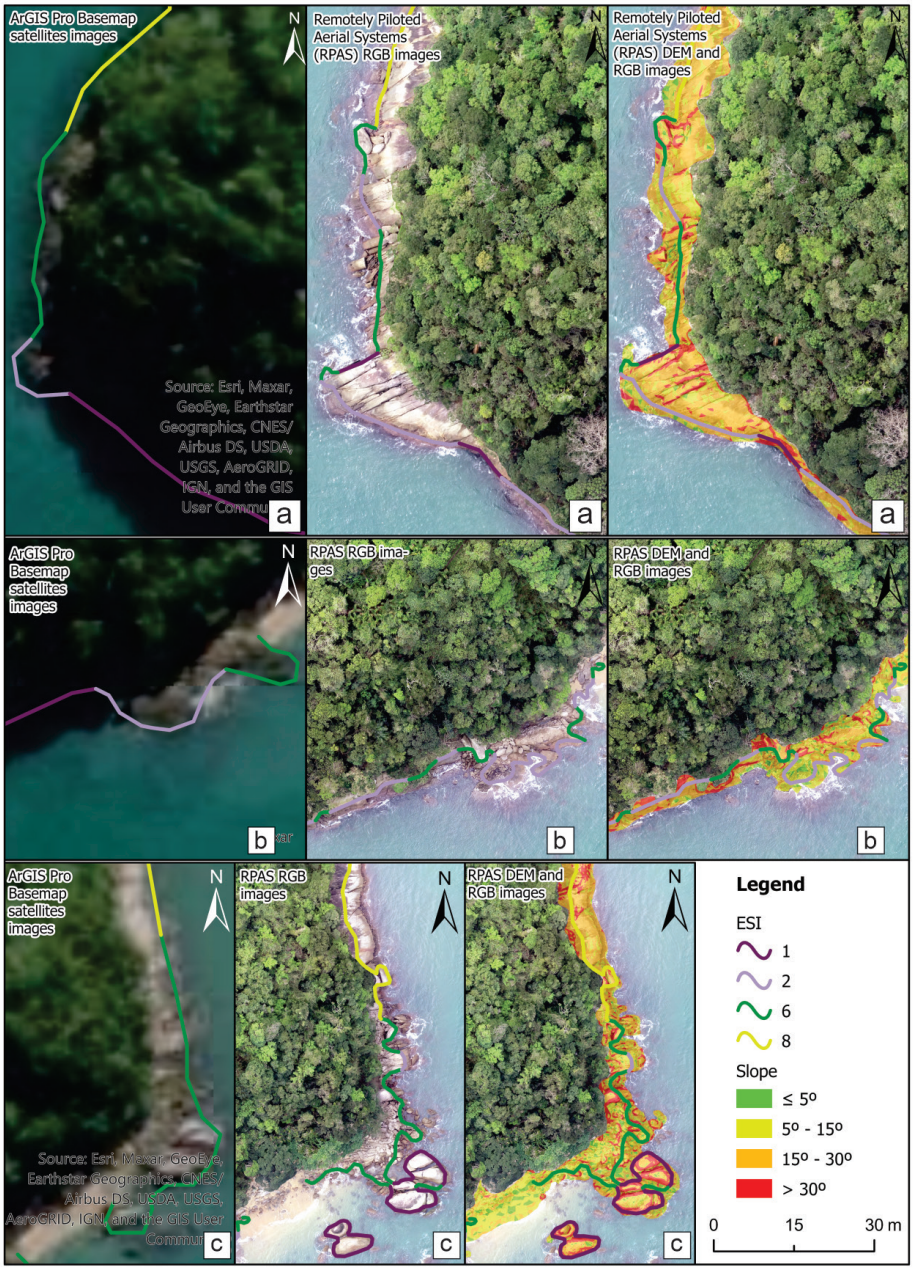

Figure 8. Interpreted ESI sections for the Cocanha Island rocky shores. From the right to the left, images from the ArcGIS Pro Basemap satellite images, Remotely Piloted Aerial Systems (RPAS) images and RPAS Digital Surface Model (DSM) superimposed on RPAS high-resolution images. Colored lines are the interpreted ESI for the rocky shores. Observe that the number of ESI section increase when RPAS images are analyzed. Figures a, b and c shows different parts of the studied area with their respective ESI analysis and slope.

the ArcGIS Pro Basemap satellite images, the influence of shadows from the trees on the rocky shores is clearly verify, making the observation and interpretation very difficult (in this case, historical images from Google Earth Pro are often used). When, for example, there is no interference from tree shadows (Figures 8b and 8c), the RPAS images increase the detail and accuracy of the ESI analysis for oil spills. Thus, it is possible to notice the compartmentalization of ESI 6 into ESI 2, due to the rectification in the interpretation of non-smooth terrains identified in the satellite images, which were unfractured or low-fractured (smooth) in the RPAS images. In the Figure 8c for example, the RPAS image clearly helped to identify the occurrence of boulders in the water (areas with ESI 1) that did not appear in the ArcGIS Pro Basemap satellite images.

The use of RPAS images is powerful when analyzing small areas, in which a detailed and high-resolution study is need. Of course, when ESI analysis is made in huge coastal regions (e.g., all the Brazilian coast) the RPAS images, despite the gain in resolution, there is a loss in sampling scale. Considering a study that covers huge areas, the RPAS images can be used to access target regions: (i) with difficult access by land, not permitting in-situ mapping; (ii) where the satellite image does not present great resolution; and (iii) with constructions and engineering installations (e.g., gas and oil stations; pipelines, refineries, etc.) that are potential sources of marine and coastal pollution. Another interesting use of RPAS images is to complement regional ESI analysis done by conventional satellite images. With the RPAS images, in areas where there is no access by land, the RPAS high-resolution images can provide significant information regarding to the physical characteristics of an environment.

CONCLUSIONS

The use of traditional remote sensing techniques, such as satellite images, are being widely used for Environmental Sensitivity Index mapping for oils spills in the Brazilian territory. However, the advancement of new remote sensing technologies, such as the Remotely Piloted Aerial Systems (RPAS), gains strength in this field of study. Herein, two rocky shores localized in two distinct areas were studied: (i) rocky shore connected to the continent ("Praia da Lagoa" Beach rocky shore) and (ii) on offshore area (Cocanha Island rocky). A comparison of the use of traditional remote sensing products (i.e., ArcGIS Pro Basemap satellite images) with RPAS images, in order to see their impact in the interpretation of these two areas in terms of Environmental Sensitivity Index (ESI) for oil spills were performed in this study.

Using RPAS images for ESI analysis of rocky shores, that offers a higher resolution and detailed compared with the ArcGIS Pro Basemap satellite images, the following can conclude:

i) the higher resolution of RPAS images offers de opportunity to increase the detailed of the ESI for oil spills, increasing the number of regions more sensitive to oil spills (Figure 8a);
ii) for the onshore rock shores ("Praia da Lagoa" Beach rocky shore), the RPAS images tend to decrease segments with the lowest values of ESI and increase those with a higher value (see Figure 7a, 7b and 7c). Using RPAS images, regions with ESI 1 highly decrease and regions with ESI 2 highly increase, same can be see for ESI 6;
iii) observing the offshore area, the Cocanha Island, the RPAS images helped to increase the detailed of the ESI analysis for oil spills, increasing the number of segments in all ESI values (see Figure 8c). Different to the "Praia

da Lagoa" Beach rocky shore, all the regions suffered from an increase of sections with a given ESI (the increase in image detailed increased the detail of ESI mapping);

iv) observing the extension of these rocky shores and the percentage of occurrence of each ESI (Tables V and VII; Figure 6), the same pattern can be traced. The occurrence of ESI 1 segments decreases while the occurrence of ESI 2 increases using RPAS images. However, for higher ESI values (ESI 6 and ESI 8), the difference between using satellite and RPAS images is very small (Figure 6);

v) the use of RPAS images, due their great detail and resolution, gives the opportunity to be more accurate in terms of declivity values (Figures 7 and 8). Since the MMA (2004), that gives guidance for ESI interpretations in Brazil, uses a visual declivity interpretation, the use of RPAS products (like de Digital Surface Model - DSM), highly increases the accuracy of the ESI and, consequently, the detailed for oil spills studies;

Notwithstanding, the use of RPAS images showed to be an interesting tool for ESI analysis for oil spills, since they have a high-resolution imaging and offers a rapid and user-friendly product for ESI interpretations. The RPAS images give a more segmented and detailed ESI interpretation, increasing the number of segments with different ESI values, so, the power in using RPAS images lies on its higher-resolution, permitting a detailed, clear and extremely visual analysis of the studied rocky shores (Figures 7 and 8). The higher resolution image offered by the RPAS (and also the temporal relation of these data) can help to identify, detail and delimit zones and ESIs that traditional remote sensing images would not be able to identify. This serves to detailed certain areas near, for example, underwater oil pipelines, refineries, ports, etc. The use of RPAS images seems to be promising in ESI analysis and interpretation for oil spills in rocky shores.

The authors also recommend that further studies should be conducted with RPAS images in other environments (mangroves, estuaries, for example) in order to understand the response of these images in different environments.

Acknowledgments

The authors thank the PETROBRAS ("Santos Project - Santos Basin Environmental Characterization", coordinated by PETROBRAS/CENPES) for scientific support and ANP (Agência Nacional do Petróleo, Gás Natural e Biocombustíveis, Brazil), associated with the investment of resources arising from the Clauses of PD&I. We also thank the "Instituto de Geociências e Ciências Exatas - IGCE" (Universidade Estadual Paulista - UNESP, Rio Claro) for providing laboratory facilities.

REFERENCES

BALL Z, ODONKOR P & CHOWDHURY S. 2017. A swarm-intelligence approach to oil spill mapping using unmanned aerial vehicles. In: AIAA Information Systems-AIAA Infotech@ Aerospace, p. 1157.

BAYIRHAN İ & GAZIOĞLU C. 2020. Use of Unmanned Aerial Vehicles (UAV) and Marine Environment Simulator in Oil Pollution Investigations. Balt J Mod Comput 8(2): 327-336.

CHIEREGATI LA, THEODOROVICZ AMG, THEODOROVICZ A, MENEZES RG, CHIODI FC & RAMALHO R. 1982. Projeto folhas Natividade da Serra e Caraguatatuba: Relatório Final, São Paulo, Companhia de Pesquisa de Recursos Minerais, Diretoria da Área de Pesquisas, Superintendência Regional de São Paulo.

COWARDIN LM, CARTER V, GOLET FC & LA ROE ET. 1979. Classification of wetlands and deepwater habitats of the United States, US Department of the Interior, Fish and Wildlife Service, Washington: DC, 131 p.

CUNLIFFE AM, BRAZIER RE & ANDERSON K. 2016. Ultra-fine grain landscape-scale quantification of dryland vegetation structure with drone-acquired structure-from-motion photogrammetry. Remote Sens Environ 183: 129-143.

DOUGHTY CL & CAVANAUGH KC. 2019. Mapping coastal wetland biomass from high resolution unmanned aerial vehicle (UAV) imagery. Remote Sens 11(5): 540.

EL MAHRAD B, NEWTON A, ICELY JD, KACIMI I, ABALANS S & SNOUSSI M. 2020. Contribution of remote sensing technologies to a holistic coastal and marine environmental management framework: A review. Remote Sens 12(14): 2313.

FREEMAN PK & FREELAND RS. 2015. Agricultural UAVs in the US: potential, policy, and hype. Remote Sens Appl: Soc Environ 2: 35-43.

GIL-AGUDELO DL, NIETO-BERNAL RA, IBARRA-MOJICA DM, GUEVARA-VARGAS AM & GUNDLACH E. 2015. Environmental sensitivity index for oil spills in marine and coastal areas in Colombia. CT&F 6(1): 17-28.

HARDIN PJ, LULLA V, JENSEN RR & JENSEN JR. 2019. Small Unmanned Aerial Systems (sUAS) for environmental remote sensing: Challenges and opportunities revisited. GIsci Remote Sens 56(2): 309-322.

HASUI Y. 2012. Sistema Orogênico Mantiqueira. Geologia do Brasil, Beca, São Paulo, p. 331-610.

HASUI Y, PONÇANO WL, BISTRICHI CA, STEIN DP, GALVÃO CACF, GIMENEZ AF & SANTOS MCSR. 1978. Geologia da região administrativa 3 (Vale do Paraíba) e parte da Região Administrativa 2 (Litoral) do estado de São Paulo: Mapa Geológico em escala 1: 200.000. Instituto de Pesquisas Tecnológicas (IPT. Monografias, 1), Publicação IPT n. 1106 (Unpublished).

HEILBRON M, PEDROSA-SOARES AC, CAMPOS NETO MDC, SILVA LD, TROUW RAJ & JANASI VDA. 2004. Província Mantiqueira. In: Mantesso-Neto V, Bartorelli A, Carneiro CD & Brito-Neves BB (Eds), Geologia do continente sul-americano: evolução da obra de Fernando Flávio Marques de Almeida, Beca, São Paulo, p. 203-235.

HODGSON JC, BAYLIS SM, MOTT R, HERROD A & CLARKE RH. 2016. Precision wildlife monitoring using unmanned aerial vehicles. Sci Rep 6(1): 1-7.

JAVADNEJAD F, SLOCUM RK, GILLINS DT, OLSEN MJ & PARRISH CE. 2021. Dense point cloud quality factor as proxy for accuracy assessment of image-based 3D reconstruction. J Surv Eng 147(1): 04020021.

JENSEN JR, HALLS JN & MICHEL J. 1998. A systems approach to Environmental Sensitivity Index (ESI) mapping for oil spill contingency planning and response. Photogramm Eng Remote Sens 64: 1003-1014.

JENSEN JR, NARUMALANI S, WEATHERBEE O, MURDAY M, SEXTON WJ & GREEN CJ. 1993. Coastal environmental sensitivity mapping for oil spills in the United Arab Emirates using remote sensing and GIS technology. Geocarto Int 8(2): 5-13.

JENSEN JR, RAMSEY III EW, HOLMES JM, MICHEL JE, SAVITSKY B & DAVIS BA. 1990. Environmental sensitivity index (ESI) mapping for oil spills using remote sensing and geographic information system technology. Int J Geogr Inf Syst 4(2): 181-201.

KANKARA RS, AROCKIARAJ S & PRABHU K. 2016. Environmental sensitivity mapping and risk assessment for oil spill along the Chennai Coast in India. Mar Pollut Bull 106(1-2): 95-103.

KLEMAS VV. 2015. Coastal and environmental remote sensing from unmanned aerial vehicles: An overview. J Coast Res 31(5): 1260-1267.

LEIGER R, APS R, KOTTA J, ORVIKU ÜK, PÄRNOJA M & TÕNISSON H. 2012. Relationship between shoreline substrate type and sensitivity of seafloor habitats at risk to oil pollution. Ocean Coast Manag 66: 12-18.

MAHDAVI S, SALEHI B, GRANGER J, AMANI M, BRISCO B & HUANG W. 2018. Remote sensing for wetland classification: A comprehensive review. GIsci Remote Sens 55(5): 623-658.

MANFREDA S ET AL. 2018. On the use of unmanned aerial systems for environmental monitoring. Remote Sens 10(4): 641.

MICHEL JM & DAHLIN J. 1993. Guidelines for developing digital environmental sensitivity index atlases and databases. US Department of Commerce, National Oceanic and Atmospheric Administration, Hazardous Materials Response and Assessment Division.

MMA - MINISTÉRIO DO MEIO AMBIENTE. 2004. Ministério do Meio Ambiente. Especificações e Normas Técnicas para Elaboração de Cartas de Sensibilidade Ambiental para Derramamentos de Óleo, 107 p.

NELSON JR & GRUBESIC TH. 2021. A spatiotemporal analysis of oil spill severity using a multi-criteria decision framework. Ocean Coast Manag 199: 105410.

NEX F & REMONDINO F. 2014. UAV for 3D mapping applications: a review. Appl Geomat 6(1): 1-15.

NIKOLAKOPOULOS K, KYRIOU A, KOUKOUVELAS I, ZYGOURI V & APOSTOLOPOULOS D. 2019. Combination of aerial, satellite, and UAV photogrammetry for mapping the diachronic coastline evolution: The case of Lefkada island. ISPRS Int J Geo-Inf 8(11): 489.

NOAA - NATIONAL OCEANIC AND ATMOSPHERIC ADMINISTRATION. 2002. Environmental Sensitivity Index Guidelines, Version 3.0. NOAA Technical Memorandum.

ODONKOR P, BALL Z & CHOWDHURY S. 2019. Distributed operation of collaborating unmanned aerial vehicles for time-sensitive oil spill mapping. Swarm Evol Comput 46: 52-68.

OYDEPO JA & ADEOFUN CO. 2011. Environmental sensitivity index mapping of Lagos shorelines. Glob Nest J 13(3): 277-287.

PETERSEN J, MICHEL J, ZENGEL S, WHITE M, LORD C & PLANK C. 2002. Environmental sensitivity index guidelines: version 3.0. National Oceanic and Atmospheric Administration, National Ocean Service, Office of Ocean Resources Conservation and Assessment Hazardous Materials Response and Assessment Division, US Dept. of Commerce, Seattle, WA, 192 p.

SANTOS CF & ANDRADE F. 2009. Environmental sensitivity of the Portuguese coast in the scope of oil spill events—comparing different assessment approaches. J Coast Res 885-889.

SOWMYA K & JAYAPPA KS. 2016. Environmental sensitivity mapping of the coast of Karnataka, west coast of India. Ocean Coast Manag 121: 70-87.

TRI DQ, DON NC, CHING CY & MISHRA PK. 2015. Application of environmental sensitivity index (ESI) maps of shorelines to coastal oil spills: a case study of Cat Ba Island, Vietnam. Environ Earth Sci 74(4): 3433-3451.

UTOMO SW, RISDIANTO RK, TAMBUNAN RP & HERNAWAN U. 2021. Environmental sensitivity index analysis for coastal protection of oil spill in Fakfak, Papua, Indonesia. Glob Nest J 23(XX): 1-8.

WAHARTE S & TRIGONI N. 2010. Supporting search and rescue operations with UAVs. In: 2010 International Conference on Emerging Security Technologies, IEEE, p. 142-147.

YANG J, GONG P, FU R, ZHANG M, CHEN J, LIANG S, XU B, SHI J & DICKINSON R. 2013. The role of satellite remote sensing in climate change studies. Nat Clim Change 3(10): 875-883.

ZHANG C & KOVACS JM. 2012. The application of small unmanned aerial systems for precision agriculture: a review. Precis Agric 13(6): 693-712.

How to cite

CERRI RI, RODRIGUES FH, DE OLIVEIRA GHS, REIS FAGV, WIECZOREK A, LONGHITANO GA & DUARTE DM. 2022. Assessing Remotely Piloted Aerial Systems in the characterization of rocky shores for oil spills environmental sensitivity mapping, northern São Paulo littoral, Brazil. An Acad Bras Cienc 94: e20210946. DOI 10.1590/0001-3765202220210946.

Manuscript received on June 29, 2021;
accepted for publication on November 13, 2021

RODRIGO I. CERRI[1]
https://orcid.org/0000-0003-3075-6100

FLÁVIO H. RODRIGUES[2]
https://orcid.org/0000-0002-2016-5334

GABRIEL H.S. DE OLIVEIRA[1]
https://orcid.org/0000-0001-9448-5763

FÁBIO A.G.V. REIS[1]
https://orcid.org/0000-0003-3918-6861

ARTHUR WIECZOREK[2]
https://orcid.org/0000-0002-4279-4617

GEORGE A. LONGHITANO[2,3]
https://orcid.org/0000-0002-1794-2518

DÉBORA M. DUARTE[3]
https://orcid.org/0000-0002-6330-1850

[1]Universidade Estadual Paulista (Unesp), Instituto de Geociências e Ciências Exatas, Departamento de Geologia, Avenida 24-A, Bela Vista, 178, 13506-900 Rio Claro, SP, Brazil

[2]Universidade Estadual Paulista (Unesp), Fundação para o Desenvolvimento da UNESP (FUNDUNESP), Instituto de Geociências e Ciências Exatas, Departamento de Geologia, Avenida 24-A, Bela Vista, 178, 13506-900 Rio Claro, SP, Brazil

[3]G Drones (Central de Soluções Profissionais), Rua Desembargador do Vale, Pompéia, 653, 05010-040 São Paulo, SP, Brazil

Correspondence to: **Rodrigo I. Cerri**
E-mail: roocerri@gmail.com

Author contributions

Rodrigo Irineu Cerri: Manuscript production and organization. RPAS and ArcGIS Pro Basemap images interpretation. Final manuscript conclusion. Flávio Henrique Rodrigues: Manuscript production and organization. RPAS and ArcGIS Pro Basemap images interpretation. Gabriel Henrique Sporh de Oliveira: RPAS and ArcGIS Pro Basemap images interpretation. Fábio Augusto Gomes Vieira Reis: Manuscript production and organization. RPAS and ArcGIS Pro Basemap images interpretation. Arthur Wieczorek: RPAS and ArcGIS Pro Basemap images interpretation. George Alfredo Longhitano: RPAS images acquisition and interpretation. Final manuscript corrections. Débora Moraes Duarte: RPAS images acquisition and interpretation. Final manuscript corrections.